IAC-18

SpaceDrive – Development of a Superconducting Levitation Thrust Balance for Propellantless Propulsion

Oliver Neunzig[a]*, Martin Tajmar[b]

[a] *Institute of Aerospace Engineering, Technische Universitaet Dresden, Marschnerstraße 32, 01062 Dresden, Germany*, oliver.neunzig@tu-dresden.de
[b] *Institute of Aerospace Engineering, Technische Universitaet Dresden, Marschnerstraße 32, 01062 Dresden, Germany*, martin.tajmar@tu-dresden.de
* Corresponding Author

Abstract

Space travel at an interstellar scale within our lifetime is a challenge primarily relying on the propulsion system of the spacecraft. Despite the continuous advancements in electrical propulsion systems, a sufficient system for this task remains to be developed. Propellantless propulsion however is believed to be the best approach towards interstellar travel. Compared to solar sails and photon rockets, the EMDrive and Mach-effect thruster are believed to excel these systems in terms of thrust. These breakthrough propulsion concepts are not yet confirmed to be functional, thus requiring the need for advanced testing facilities. To investigate these concepts amongst others at the Institute of Aerospace Engineering at Technische Universität Dresden (TU Dresden), a new kind of rotational thrust balance was designed. By measuring the change in angular velocity of a magnetically levitated system inside a vacuum chamber onto which the thrusters apply a torque, thrusts in the range of ~1 µN will be detected. Goal of the thrust balance is to reduce the probability of false measurements due to interactions between the thrusters and the environment, such as earth's magnetic field or vibrations through the balance components. Therefore, the balance is based on a magnetic levitation bearing utilizing high-temperature superconductors and permanent magnets to provide a frictionless rotational degree of freedom. Measurements of the levitation force resulted in a maximum axial load capability of 22 kg for the magnetic bearing, which is an order of magnitude above electromagnetically levitated thrust balances. Preliminary experimental setups of superconducting bearings on a smaller scale have been analyzed at atmospheric pressure towards frictional torque at angular velocities below 0.5 rad/s. The measured torque of 2.4x10e-6 Nm contains a decreasing tendency for a vacuum environment. The facility will feature a high precision optical sensor to track its angular position in order to derive the actual thrust force along its trajectory. Liquid-metal contacts will provide on-board power as well as data acquisition. A levelling mechanism will be able to adjust the centre of mass of the levitating system in order to enable full rotations for the thrusters. The facility will provide a space-like friction-free environment to test propellanteless propulsion concepts as well as complete Nanosatellites.

Keywords: Thrust balance, Thrust measurement, Superconductor, Magnetic Levitation, Propellantless propulsion

Nomenclature

Δv	-	Change in velocity [m/s]
T_C	-	Critical temperature [K]
J_C	-	Critical current density [A/m²]
B_C	-	Critical magnetic flux density [T]
M_T	-	Torque of the propulsion system [Nm]
F_T	-	Thrust of the propulsion system [N]
R	-	Thruster lever-arm [m]
J	-	Moment of inertia [kgm²]
a	-	Angular acceleration [rad/s²]
$\Delta\omega$	-	Change in angular velocity [rad/s]
Δt	-	Time of thruster operation [s]
$\vec{g}$	-	Gravitational acceleration [m/s²]
$\vec{a}$	-	Fractional acceleration [m/s²]
i	-	Rotational plane inclination [rad]
$F_{\vec{a},COM}$		Fractional gravitational force [N]
F_D	-	Fluid resistance [N]
C_D	-	Drag coefficient
ρ	-	Fluid density [kg/m³]
v	-	Velocity of the contacts [m/s]
A	-	Area against the flow [m²]

Acronyms/Abbreviations

YBCO - Yttrium barium copper oxide
DOF - Degree of freedom
SC - Superconductor
FCD - Field cooling distance

1. Introduction

Modern space travel is confronted with a ceaseless desire of mankind to explore the universe beyond our solar system. To lay the foundation for interstellar missions within our lifetime, the development of new technologies for the main challenges of this intention are inevitable. Since space travel primarily relies on overcoming enormous distances, there are strong technical requirements for propulsion technologies. Despite continuous advancements in space propulsion systems, present systems no longer meet the desired performances for large-scale missions. Sir Isaac

Newton's third law of motion and the Tsiolkowsky's rocket-equation confine their realm of feasibility towards large Δv with on-board propellant. There is a strong need for a breakthrough in propulsion physics.

A novel approach for this challenge are propellantless propulsion concepts. Systems like solar sails and beamed laser propulsion [1], that utilize radiation pressure of the sun or lasers from earth, do not rely on stored propellant. However, they are constricted due to their extrinsic source of energy. The EMDrive [2],[3] and Mach-effect thruster [4],[5] are believed to excel these systems in terms of thrust neither by relying on external energy sources nor on-board propellant to propel a spacecraft. Unlike solar sails, these concepts are not yet confirmed to be functional, but they could lead to a breakthrough in propulsion physics. Within the SpaceDrive project at the Institute of Aerospace Engineering at TU Dresden thorough investigations of these systems demand advanced testing facilities. With a precise torsional balance thrusts in the range of µN have been observed for the EMDrive, that could be subject to false measurements due to interactions with earths' magnetic field [6],[7].

To verify measurement artefacts and reduce the probability of false measurements, a new kind of rotational thrust balance was designed and is presented in this paper (Fig. 1).

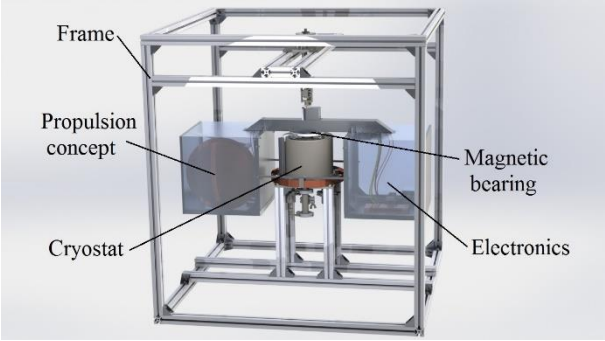

Fig. 1. Rotational thrust balance developed at the Institute of Aerospace Engineering at TU Dresden.

By measuring the change in angular velocity of a frictionless circular trajectory, thrusts in the range of 1 µN can be calculated. The difficulty in providing movements of large masses with forces in the range of ~µN is friction within the bearing. Components like ball bearings are still orders of magnitude above the tolerable frictional forces and therefore unsuitable. To overcome this issue, the balance is based on magnetic levitation. A notable example of a magnetically levitated thrust balance is the system developed by Mier-Hicks and Lorenzo [8]. Their approach is an electromagnetically levitated balance for CubeSats with Electrospray thrusters, which is capable of ~µN thrust measurements for a levitated mass of up to 1 kg.

The rotational thrust balance presented in this paper is designed for a thrust measurement range of 1 µN while it is able to levitate a mass of up to 22 kg. The balance utilizes the unique properties of superconductivity, discovered by H. K. Onnes in 1911 [9] with first hypotheses of its quantum mechanical origin explained in the BCS-Theory [10] by J. Bardeen, L. Cooper and R. Schrieffer with the formation of cooper-pairs.

The superconducting material-combination of Yttrium-Barium-Copper-Oxide (YBCO), which loses its electrical resistivity at 92 K in combination with a cylindrical permanent magnet will be utilized to passively levitate propulsion concepts and perform full rotations. To access the superconducting properties of YBCO over a long period, the facility features a cryostat with a liquid-nitrogen heat exchanger, presented in chapter 2.2.2.

Determined by the combined properties of cylindrical permanent magnets and superconductors to retain one remaining degree of freedom, the rotational plane of the balance has to be levelled below a threshold of 0.01° to enable full rotations of a levitated mass of 22 kg with only 1µN of thrust. A detailed description of the levelling procedure prior to measurements is presented in chapter 2.3. Additionally, this paper provides information on the thrust measurement principle with highly precise angular sensors (Chapter 3.1) as well as frictional torque measurements (chapter 4.1), flux density measurements (chapter 4.2) and levitation force capacities of the magnetic bearing (chapter 4.3).

2. Material and methods

The thrust balance is designed to magnetically levitate a propulsion concept of interest and the supporting frame with a total mass of up to 22 kg inside a vacuum chamber. In order to provide full rotations for the thruster with expected thrust forces in the range of µN, the rotating plane of the circulator trajectory must not exceed a deviation from the perfect level of 0.01°. For this reason, the facility features a holding-mechanism with a double pivot-bearing, allowing pendulum like movements in two axis (Fig. 2).

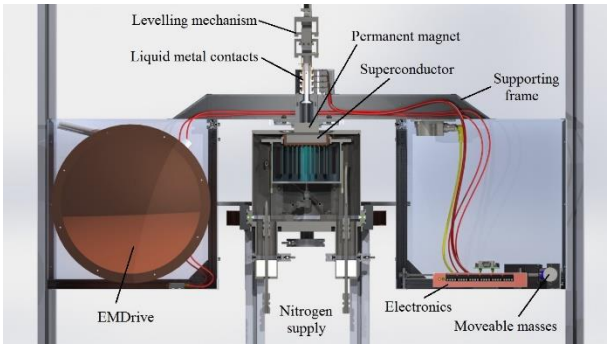

Fig. 2. Sectional view of the magnetically levitated structure and the cryostat

With moveable masses inside the electronics box, the centre of mass of the levitating frame can be adjusted to fit the requirements for a full rotation. An inclination sensor on the main supporting beam provides telemetric data to observe the levelling process.

The main parts of the magnetic bearing are a cylindrical permanent magnet and a superconductor inside a cryostat with a reservoir of liquid nitrogen. The bearing enables almost zero-friction along a single rotational degree of freedom. With liquid metal contacts, the electronics and thruster can be supplied with electrical power while performing full rotations. A high precision optical sensor tracks its angular position in order to derive the actual thrust force along its trajectory. The following sub-sections will provide a detailed look at the main parts of the balance.

2.1 Support frame and Thruster containment

The total load capacity of the magnetic levitation bearing had to be taken into account for selecting materials for the structural parts of the balance. To design the structure as lightweight as possible, thus providing a large margin for the thruster weight, the supporting frame and containments for thruster and electronics are made of lightweight aluminium profiles. The middle aluminium beam contains the cable management from the liquid metal contacts to the electronics and thruster containment. To create a sufficient resistance against the bending moment of the thruster weight, the beam features a wall thickness of 3 mm and a rectangular profile. While reinforcing the structure, the aluminium containments around the electronics and the thruster act as a faraday-cage to shield any electrostatic interactions between the electronics and the environment inside the vacuum chamber (Fig. 3). Otherwise, these interactions may lead to measurement errors.

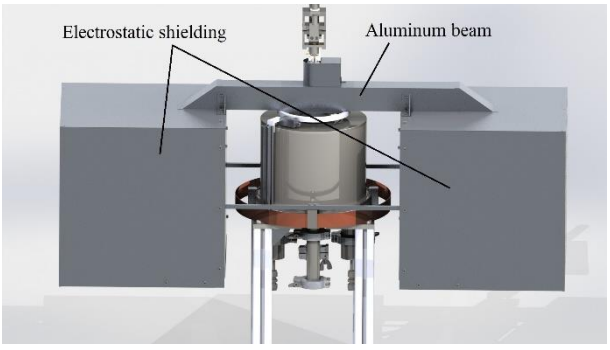

Fig. 3. Thrust balance (side-view) with aluminium containments for electrostatic shielding.

The magnetic field of the permanent magnet is very sensible towards magnetic materials in close vicinities. Distortions of the magnetic field lines could lead to complications during measurements. For that reason, every part of the thrust balance is made of either stainless steel and aluminium or other non-magnetic materials like PEEK and copper.

While not cooled below a temperature of 92 K, the superconductor does not interact with the permanent magnet whatsoever, thus disabling the magnetic levitation. During these phases, the rotating part of the balance supported by a mechanism that is fixated to a frame and surrounds the whole balance. This frame is made of rigid 40x40 mm aluminium beams and represents the balance basis inside the vacuum chamber.

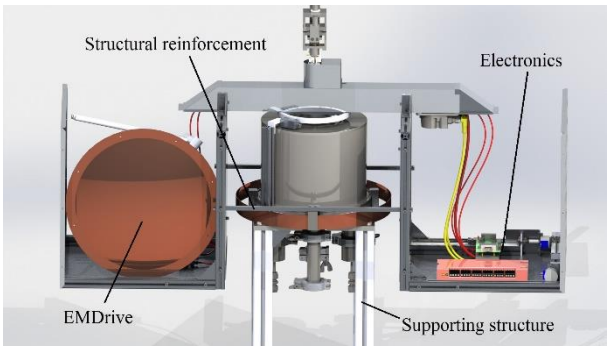

Fig. 4. Thrust balance (side view) with uncovered containments to gain access to the propulsion system and electronics.

2.2 Magnetic bearing

Providing circular movements of the levitated mass with ~µN of thrust strongly depends on the bearing of the system. The frictional torque of components like ball bearings is magnitudes above the tolerable friction for the balance. So far, the best approach towards zero friction is a system with magnetically levitated components. System of choice is a combination of a cylindrical NeFeB permanent magnet and an Yttrium-Barium-Copper-Oxide high-temperature superconductor disc. This combination is commonly used for high-speed rotational applications like energy storage in flywheels with minimal energy losses due to the low frictional torque. The permanent magnet has an outer diameter of 50 mm and a height of 20 mm with a quality specification of N50, thus providing an approximated energy product 50 MGOe. Two different sizes of YBCO high-temperature superconductors are available for the balance. Both of which with a height of 16 mm and outer diameters of 54 mm/80 mm. YBCO has a critical temperature of 92 K that needs to be reached in order to access the superconducting properties. This type of bearing is able to provide an axial load capacity of up to 22 kg while maintaining one rotational degree of freedom with almost zero-friction. The basic functional principle of the magnetic levitation is presented in figure 5.

The superconductor is submerged within a bath of liquid nitrogen to reduce its temperature to -196°C while the permanent magnet passively levitates above. In

comparison to electromagnetically levitated magnets, this system offers an increased axial load capacity on a smaller construction volume, while not depending on closed-loop control of the electromagnetic coil. Downside of the superconducting levitation is an increased constructional complexity for a cryostat in order to keep the superconductor below its critical temperature.

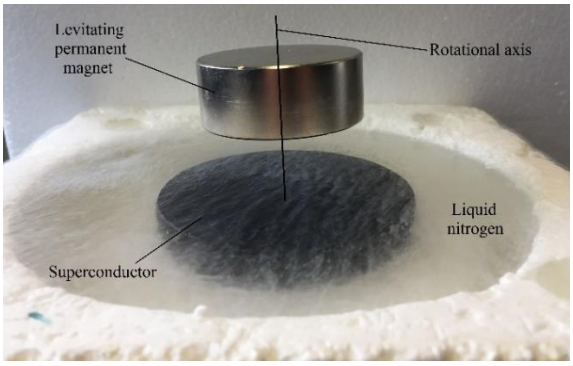

Fig. 5. Levitating permanent magnet above an YBCO superconductor submerged within liquid nitrogen.

2.2.1 YBCO High-temperature superconductor

As mentioned before, a superconductor below its critical temperature has the ability to conduct electrical currents without resistivity whatsoever. This property leads to unique electromagnetic interactions with external magnetic fields. If a superconductor is cooled below its critical temperature in presence of an external magnetic field from a permanent magnet, it acts like a magnetic mirror. The material combination of YBCO belongs to the class of type II high-temperature superconductors. The properties of this type can be divided into three main characteristics during the cooling process (Fig. 6).

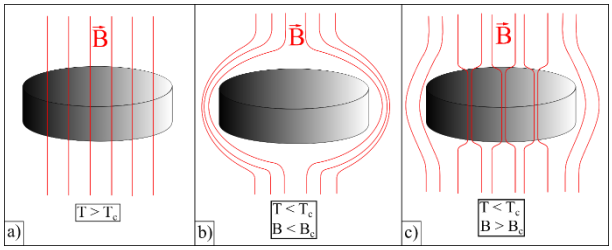

Fig. 6. Properties of a Type-II Superconductor: a) above the critical temperature (Normal phase); b) below the critical temperature (Meissner state); c) above the critical magnetic flux density (vortex phase).

While the superconductor is above its critical temperature (Fig 6, a), there are no interactions with external magnetic fields and the SC. In phase two of the cooling process, the SC reaches its critical temperature T_C , hence enabling the superconducting properties. As long as the maximum current density j_C inside the SC is not exceeded, the SC stays in this so-called Meissner-state and repels any external magnetic fields from its core (Fig 6, b). If the external magnetic field exceeds a critical flux density B_C , the current density of the superconductor surpasses its critical limit and reacts with the formation of so-called flux tubes (Fig. 6, c). At these positions, the magnetic field penetrates the SC and locks the magnetic field in position through the generation of flux vortices in the vortex-phase [11]. In this state, cylindrical permanent magnets are magnetically restricted in their motion by solely leaving a rotational degree of freedom and creating a spring-like stiffness in radial and axial direction, that increases with lower temperatures. The rotational DOF remains due to the rotationally symmetric magnetic field lines from the cylindrical magnet. The axial force of the superconductor strongly depends on the distance between the SC and the magnet while reaching the critical temperature. This distance is defined as the field cooling distance (FCD).

The superconductor on its own does not withstand multiple load cycles. The material has to be strengthened due to a high sensitivity towards bending moments. A thin layer of a two-component adhesive called *STYCAST* reinforces the mechanical structure of the SC and prevents it from outgassing and degrading its properties.

2.2.2 Cryostat

To access the superconducting properties of Yttrium-barium-copper-oxide over a long period, the material requires a continuous cooling below its characteristic critical temperature of 92 K. For this reason, the system features a liquid nitrogen cryostat. In general, this device contains a heat exchanger of various shapes and thermal insulation techniques to reduce the required amount of energy. There are three distinct function principles commonly used for cryostats, like the flow-cycle and bath cryostat that utilize liquid nitrogen as a cooling medium. On the other hand there are systems like cryocoolers, that obtain cryogenic temperatures with a refrigerating process. The thrust balance presented in this paper features a heat exchanger with a liquid nitrogen bath-cryostat (Fig. 7).

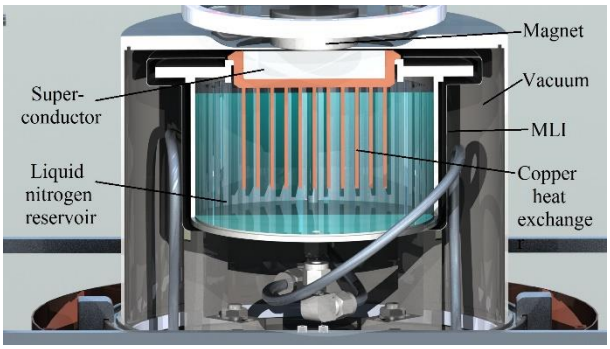

Fig. 7. Sectional view of the cryostat with the liquid nitrogen heat exchanger within a vacuum containment.

Two fabric tubes supply the reservoir with liquid nitrogen through ascension tubes. The reservoir itself is a welded stainless steel containment with a copper cold head, which is hard-soldered into the cover-plate. Two superconductors of different sizes are positioned within the cold head and fixated with a copper socket. Eleven copper plates are hard-soldered to the underpart of the cold head and immersed into the liquid nitrogen. This arrangement exchanges the heat from the superconductor with the liquid nitrogen to cool it below its critical temperature.

At 1 bar of atmospheric pressure liquid nitrogen evaporates due to the absorbed heat of the surrounding materials. To prevent the containment from exceeding its pressure limits the evaporated nitrogen exits through one of the supply tubes. Exposed to 1 Bar of atmospheric pressure, liquid nitrogen boils at a temperature of 77 K. By lowering the atmospheric pressure inside the nitrogen reservoir with a vacuum pump, the boiling temperature reaches a minimum of 63 K while it undergoes a phase-change from liquid to solid. With this enhancement, the temperature of the superconductor further decreases, which leads to an improved levitating force and radial stiffness of the bearing.

The reservoir is covered in multi-layer-insulation to minimize heat losses through radiation. A stainless steel housing around the superconductor and liquid nitrogen reservoir can be depressurised in order to reduce heat losses due to convection. This enhancement provides the ability for tests outside of the vacuum chamber by protecting the components from air exposition and the formation of ice on cold surfaces due to humidity.

To handle the axial load of the levitating structure of up to 22 kg, the reservoir is reinforced with four supporting pillars that are fixated to the external frame. A large section of these pillars is made of PEEK. This material features a large tensile strength at cryogenic temperature while reducing heat losses through thermal conduction.

2.3 Hold-and-Release mechanism

A precise alignment of the permanent magnet and the superconductor in terms of field cooling distance and coaxial orientation has to be conducted prior to the measurements. Due to operations inside a vacuum chamber, this alignment-process requires remote-controlled positioning systems. For this reason, the facility features an adjustable mechanism that consists of a leading screw on a spindle to adjust the FCD with a stepper-motor and regulate the desired parameters (Fig. 7).

A system with one degree of freedom constrains its self-levelling ability and depends on active adjustments. Therefore, the levitating structure is levelled with inclination sensors and moveable masses.

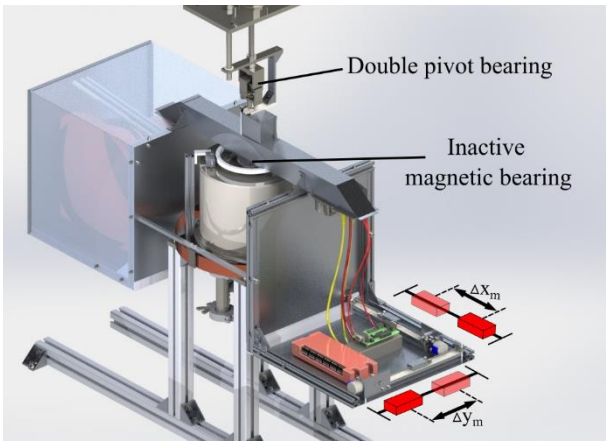

Fig. 7. Levelling-mechanism with moveable masses, controlled with stepper motors inside the electronics-containment.

For this reason, the spindle in mounted onto a double pivot bearing to make sure, that the structure is able to align its centre of mass within the rotational axis. Two moveable masses inside the electronics box can be adjusted with stepper motors to manipulate the centre of mass of the levitating structure. Thereby, the rotational plane can be levelled to the desired value (Fig. 8).

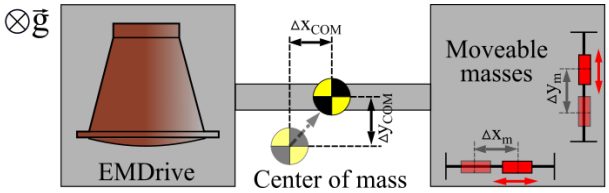

Fig. 8. Functional principle for adjustments of the centre of mass with moveable masses inside the electronics-containment.

An inclination sensor with a resolution of 0.01° observes the inclination of the rotational plane while adjusting the centre of mass.

After the levelling process inside the vacuum chamber, the next step is to enable the magnetic levitation by cooling the superconductor with liquid nitrogen below its critical temperature. Subsequently, the spindle mechanism is lowered until the gravitational force of the levitating system is completely transferred to the magnetic levitation force. At this point, the holding mechanism loses contact with the rotating components and the balance is prepared for operations.

2.4 Electrical power supply

In order to operate the thrusters and electronics, electrical energy must be delivered to the balance. Measuring small movements of the balance as a result of thrust is very sensible towards any kind of stiff connections and wires to the frame. Every wire from the

power supplies to the propulsion system disturbs measurements by preventing deflections due to stiffness of the wire materials. To counteract this problem, the balance features a power feedthrough utilizing a metal alloy called Galinstan, which is liquid at room temperature and exhibits a very low vapour pressure. The rotationally symmetric containments made from PEEK are positioned above each other as close as possible to the rotational axis of the system and fixated externally. Copper-pins from the rotating frame are submerged inside the Galinstan to provide on-board power as well as data acquisition (Fig. 9).

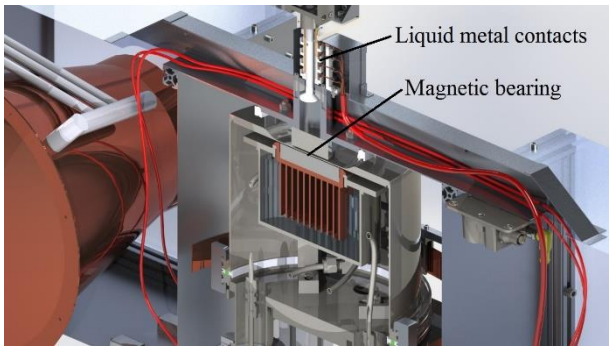

Fig. 9. Liquid metal contacts in the rotational axis to supply the propulsion system with electrical power while performing rotations.

As a consequence of the moving pins inside the liquid metal during rotations, liquid friction is induced to the measurements. This friction strongly depends on the lever arm of the copper pins and the angular velocity, upon which the fluid friction scales. This frictional component has to be quantified and considered in the thrust measurements. A more detailed view of the liquid metal contacts is presented in figure 10.

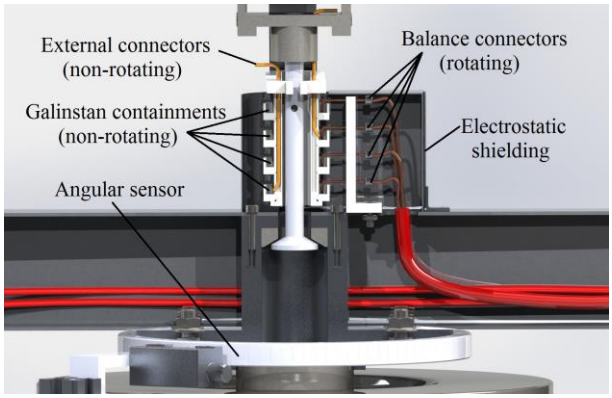

Fig. 10. Sectional view of the liquid metal contacts in the rotational axis of the magnetic bearing.

2.5 Damping system

Whilst maintaining the zero friction environment of the levitating structure inside the vacuum chamber, any amount of acquired angular momentum leads to a rotation of the system. To counteract this motion during alignments or decelerations of the levitated structure, a controllable damping system will be installed to the balance. Two electromagnets with iron cores are fixated to the non-rotating part of the balance. A circular sheet of copper is fixated to the rotating structure and moves in close distance to the electromagnet. Any form of magnetic field originating from the electromagnets, penetrates the copper plate. If the electromagnet and the copper plate are at rest with respect to each other, this system has no influence on the movement whatsoever. Any motion of the plate induces electrical currents within the copper plate perpendicular to the magnetic field lines of the electromagnet due to Faraday's law of induction. These eddy-currents lead to damping forces, counteracting unwanted movements of the levitated structure.

2.6 Angular sensor

In order to derive the actual force of the thruster along its trajectory, the balance will feature a high precision optical sensor to track its angular position without contact. The *Resolute UHV system* consists of a stainless steel ring with a single track of µm-cuts inside the metal that are analyzed by an absolute optical encoder. The ring will be positioned on the rotating frame whilst the encoder captures displacements in the range of micrometres (Fig. 11).

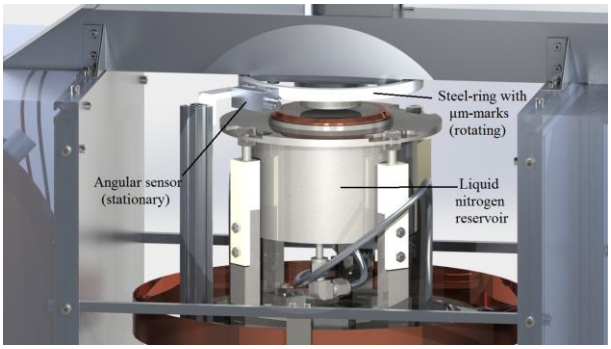

Fig. 11. Position of the high precision angular sensor in the rotational axis of the magnetic bearing.

3. Theory and calculation

3.1 Thrust measurement principle

After the balance is placed under vacuum conditions, the thrust measurement sequence will proceed as follows. At first the magnetic levitation is not yet enabled in order to level the rotational plane of the circular trajectory. A more precise explanation of this step is explained in chapter 3.4. Subsequently, the superconductor is cooled below its critical temperature by filling the reservoir with liquid nitrogen. After magnetic levitation is acquired, the levelling mechanism can be disabled and removed from

the levitating structure, hence enabling the friction free rotational degree of freedom. The propulsion system applies a force onto the levitating thruster at lever-arm R, which leads to a torque onto the magnetic bearing (Fig. 12.).

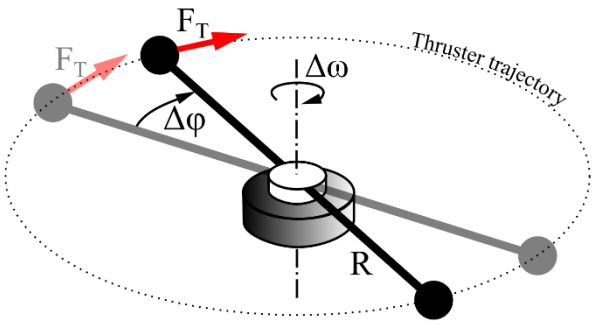

Fig. 12.Thrust measurement principle of the propulsion system along a circular trajectory

Any gain in angular velocity will be detected by the angular sensor with a resolution of 1 µm. In an ideal frictionless environment, basic physics is needed to calculate the produced thrust by knowing the moment of inertia of the levitated structure J, the gain in angular velocity $\Delta\omega$, thruster lever arm R and the amount of time Δt of thruster operations. The thrust is then calculated by using equations (1)-(3).

$$M_T = F_T \cdot R = J \cdot a \qquad (1)$$

$$a = \frac{\Delta\omega}{\Delta t} \qquad (2)$$

$$F_T = \frac{J \cdot \Delta\omega}{R \cdot \Delta t} \qquad (3)$$

It is important to notice, that the non-ideal rotational behaviour includes disturbing factors, that have to be taken into account during measurements regarding frictional torque. The performance of the magnetic bearing is constrained by the quality of the superconductor and permanent magnet. Either of which could possess inhomogeneities in their flux density distribution across their surfaces. These inhomogeneities could lead to magnetic forces that interfere thrust measurements. For this reason, the magnetic flux densities of the bearing parts have been measured experimentally and are presented in chapter 4.2.

3.2 Inclination of the rotational plane

There is a significant dependency between the ability to perform full rotations and the inclination of the corresponding rotational plane. Insufficient alignments of the centre of mass of the levitating structure lead to complications in thrust measurements by introducing a scaling fraction of the gravitational acceleration within the rotational plane. This fraction interferes with the measurements by preventing full rotations due to a restoring gravitational force that scales with the levitated mass and the inclination. Critical misalignments of levitated masses up to 22 kg may prevent any rotations whatsoever.

As mentioned before, the absence of the bearings self-levelling ability and the resolution of the inclination sensor are limiting the minimum value of the gravitational fraction according to equation (4).

$$\vec{a} = \vec{g} \cdot \sin(i) \qquad (4)$$

This relation is described in figure 13 with a lateral view of the rotational plane. The positions 1-4 indicate different positions of the centre of mass that will be used to describe its influence on thrust measurements within this chapter.

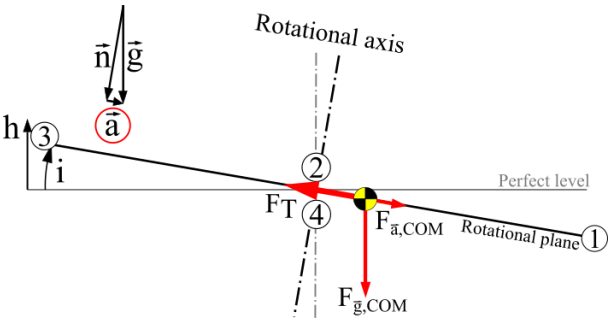

Fig. 13. Misalignments of the rotational plane lead to a scaling gravitational force counteracting the thrust originating from the propulsion system.

Thrust measurements will take place either by averaging the thrust for the total sum of rotations in time or by analysing one isolated rotation. In the case of thrusts close to the resolution of the balance, it is beneficial to derive the continuous thrust by small deflections rather than full rotations. Therefore, the rotational plane has to be dissected into four different quadrants, either of which with a different influence of the rotational plane inclination (Fig. 14)

In quadrants I-II the fraction of the gravitational force $F_{\vec{a},COM}$ opposes the thrust F_T provided by the propulsion system, hence slowing the circular motion. In quadrants III-IV the gravitational force supports the angular velocity. Position 1 indicates the resting position of the centre of Mass, where the rotational plane is at its lowermost position within the gravitational field (h=minimum). This position is a stable equilibrium between gravitational force of the centre of mass due to the fractional amount of gravitational acceleration A and the inclination of the rotational plane. Positions 2 and 4 exhibit the largest influence in thrust measurements due to a maximum in restoring torque, that counteracts the thrust vector of the propulsion system. Especially

location 2 determines the minimum thrust for a full rotation, because gravitational torque is at its maximum. Similar to position 1, the location indicated with 3 is an equilibrium at the highest position within the gravitational field, therefore it is unstable.

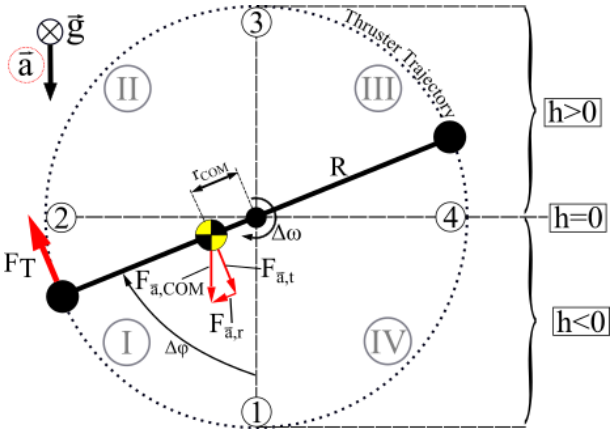

Fig. 14. Different influences of the misaligned rotational plane in four quadrants of a full rotation.

These constraints of measurements in the lower thrust range fortify the importance of rotational plane levelling. Due to the high-resolution angular sensor, these dependencies will be measurable

3.3 Influence of fluidfriction in Galinstan

The constraint of continuous power supply to the balance while performing rotations leads to an influence in measurements. The liquid metal contacts supply electrical energy during rotations while being submerged within the liquid metal. This is the only direct contact between the rotating system and the external frame, besides the magnetic repulsion from the superconductor. Therefore, fluid friction was introduced to the thrust equations by calculating the drag of each contact. Under the assumption of a Newtonian fluid with a linear viscosity and laminar flow due to small Reynolds-numbers, the fluid resistance was approximated with equation (5).

$$F_D = c_D \frac{\rho}{2} v^2 A \quad (5)$$

These calculations are first approximations of the drag that have to be validated prior to thrust measurements by analysing their influence in angular velocities.

4. Results

4.1 Frictional torque measurements of the bearing

Most practical applications of superconducting bearings are designed for high rotational velocities, therefore an analysis of low rotational speeds had to be performed prior to the thrust balance development. Preliminary experimental setups of superconducting bearings on a smaller scale have been analyzed at atmospheric pressure towards frictional torque at angular velocities below 0.5 rad/s. A comparable magnetic bearing, featuring a superconductor and a levitating permanent magnet was used for the test. An initial impulse lead to a circular motion of the levitated structure. With the loss in kinetic energy of each rotation, a frictional torque in steps of half rotations was calculated and is presented in figure 15.

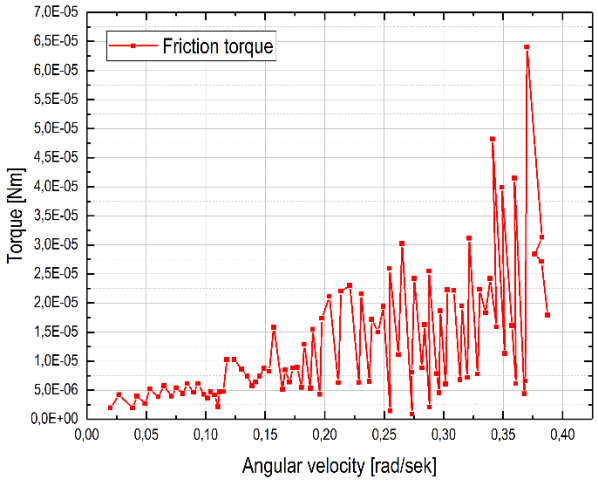

Fig. 15. Frictional torque calculations of a rotating structure that is passively levitated with a superconductor at atmospheric pressure.

The measured torque reached a minimum value of 2.4x10e-6 Nm for an angular velocity of 0.02 rad/s. As a result of the non-vacuum environment, the influence of atmospheric drag could not be excluded during the experiment. Nevertheless, the experimental results contain a decreasing tendency of frictional torque for a vacuum environment.

4.2 Flux density measurements

In order to evaluate the importance of inhomogeneities within the superconductors and the magnet, that arised during manufacturing processes, measurements of the trapped flux density inside the superconductor were conducted.

The flux density measurements were performed by positioning a cylindrical permanent magnet near the superconductor in a field cooling distance of 5 mm. By cooling the SC below its critical temperature with liquid nitrogen, the magnetic field of the permanent magnet was mirrored inside the SC. At this point, the magnet was locked in position by the superconductor and had to be removed mechanically. Without interrupting the cooling process, the mirrored field remained inside the SC. Subsequently, the magnetic field was measured with a hall sensor and processed in pseudo-color to inspect the

trapped flux densities. This procedure was conducted with two available cylindrical superconductors with the same height, but different radii of 54mm (Fig 16) and 80mm (Fig. 17).

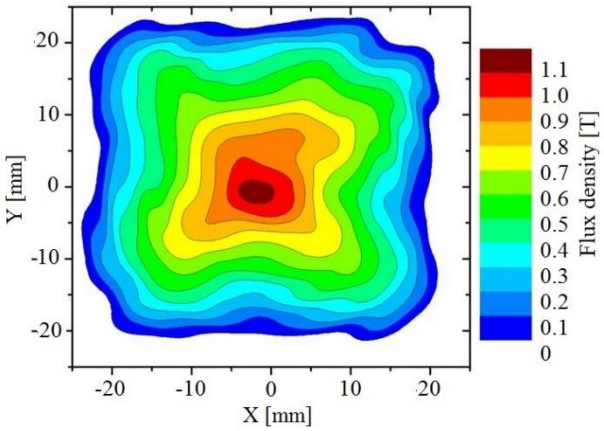

Fig. 16. Magnetic flux density of a superconductor with geometric dimensions of 16 mm in height and 54 mm in diameter.

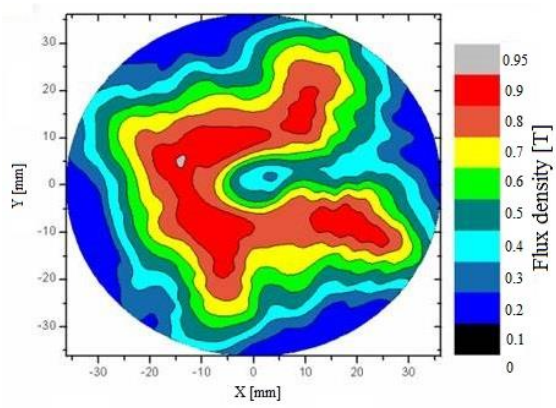

Fig. 17. Magnetic flux density of a superconductor with geometric dimensions of 16 mm in height and 80 mm in diameter.

As a result of difficult circumstances in the manufacturing process of large superconductors, the specimen with an outer diameter of 80 mm contains strong inhomogeneities regarding the trapped magnetic flux density. The smaller superconductor offers a far better magnetic flux distribution, thus offering better performance for the frictionless rotation, but at cost of axial load capacity. The reduced surface area of the small SC does offer the same load capacity as the large specimen, because there are not as much magnetic field lines trapped within the SC. Nevertheless, the axial force is still dependant on the size and quality of the permanent magnet. Therefore, the permanent magnet was measured as well regarding its magnetic flux distribution long the surface (Fig. 18). The results lead to the conclusion, that it overall provides a decently homogenous magnetic flux distribution.

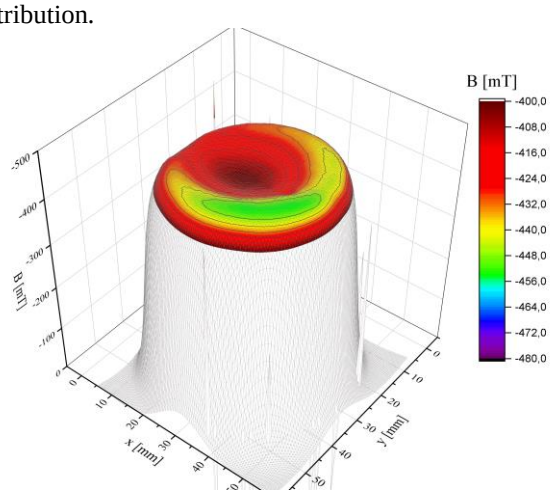

Fig 18. Flux density surface distribution of a permanent magnet with geometric dimensions of 20 mm in height and 50 mm in diameter.

The slight drop in measured density originates from a misalignment of the magnet within the measurement apparatus. The magnetic axis includes a slight deviation of the symmetrical axis, which potentially leads to misalignments during the levelling of the rotating frame. The deviation was analysed and considered in the geometric tolerances of the socket of the magnet on the thrust balance.

4.3 Levitation force measurement

Although the frictional torque of the rotational DOF is the most important characteristic of the magnetic bearing, there is another factor involved in its capabilities. The axial magnetic force of the superconductor constrains the maximum combined weight of the propulsion system and the structural mass. Therefore, axial magnetic force measurements have been conducted with both YBCO superconductors in combination with the cylindrical permanent magnet.

For this process, the superconductor was cooled below its critical temperature without external magnetic fields in close proximity. This so-called zero-field-cooling procedure enables the superconducting Meissner-state, hence repelling external magnetic fields from its core. With a testing-facility, the permanent magnet was forced to a distance down to 1 mm towards the SC and returning to the initial position while analysing the needed force for each distance. As seen in figure 19, there is a squared dependency of the magnetic force and the distance between the components, reaching a maximum axial force of 250 N at a distance of 1 mm. The same procedure was conducted with a field-cooling height of 30 mm, leading to a slight decrease in the maximum axial force of 220 N, thus constraining the limits of the levitating structure to 22 kg.

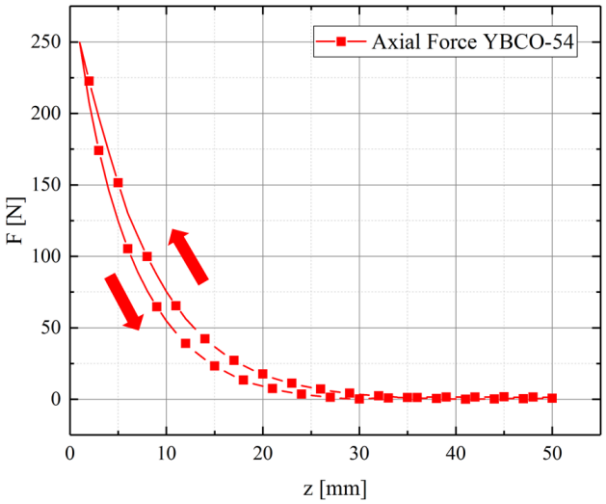

Fig. 19. Levitation force measurement of the superconductor for distances down to 1 mm between the superconductor and the permanent magnet.

5. Conclusions and further work

A rotational thrust balances for propellantless propulsion concepts and Nanosats was developed at the Institute of Aerospace Engineering at TU Dresden. The balance is designed to measure thrust in the range of 1 µN by analysing the change in angular acceleration of a magnetically levitated structure. A passive magnetic bearing with YBCO high-temperature superconductors and permanent magnets offer a close to zero frictional torque to enable full rotations along a circular trajectory inside a vacuum chamber.

Thrust measurement principles with adjustments for gravitational influences in the rotational plain were described.

Levitation force measurements of the magnetic bearing resulted in a maximum load capacity of 22 kg for the total levitated mass. This value may be further improved by varying the size, quality and field-cooling distance of the permanent magnets. The influence of inhomogeneities within the magnetic bearing components has been evaluated with magnetic flux density measurements of the superconductors and permanent magnets. According to the measurements, there is a discrepancy in terms of quality between the two available superconductors, therefore enhanced characteristics of the smaller SC are expected.

Properties of the levitating thrust balance in total are not yet characterized, but expectations towards frictional torque have been analysed with a superconducting levitation bearing on a smaller scale.

Due to the adaptable design of the balance, a wide variety of propulsion systems that do not rely on external propellant supply will be tested.

Acknowledgements

We gratefully acknowledge the support for the SpaceDrive project by the German national space Agency DLR (Deutsches Zentrum fuer Luft- und Raumfahrttechnik) by funding from the Federal Ministry of Economic Affairs and Energy (BMWi) by approval from German Parliament (50RS1704).

Furthermore, we want to thank the Leibniz Institute for Solid State and Materials Research Dresden and especially T. Espenhahn for providing access to their testing facilities.

References

[1] M. Tajmar: *Advanced Space Propulsion Systems*, Springer Vienna, 2003

[2] Tajmar, M., and Fiedler, G., "Direct Thrust Measurements of an EMDrive and Evaluation of Possible Side-Effects," *51st AIAA/SAE/ASEE Joint Propulsion Conference*, 2015, p. AIAA 2015-4083. doi:10.2514/6.2015-4083

[3] Shawyer, R., "Second Generation EmDrive Propulsion Applied to SSTO Launcher and Interstellar Probe," *Acta Astronautica*, vol. 116, 2015, pp. 166–174. doi:10.1016/j.actaastro.2015.07.002

[4] Woodward, J. F., "A New Experimental Approach to Mach's Principle and Relativistic Graviation," *Foundations of Physics Letters*, vol. 3, Oct. 1990, pp. 497–506. doi:10.1007/BF00665932

[5] Fearn, H., Zachar, A., Wanser, K., and Woodward, J., "Theory of a Mach Effect Thruster I," *Journal of Modern Physics*, vol. 6, 2015, pp. 1510–1525. doi:10.4236/jmp.2015.611155

[6] M. Tajmar, M. Kößling, M. Weikert, M. Monette, *The SpaceDrive Project - Developing Revolutionary Propulsion at TU Dresden*, International Astronautical Congress, 2017.

[7] M. Tajmar, M. Kößling, M. Weikert, M. Monette, *The SpacDrive Project – First Results on EMDrive and Mach-Effect Thruster*, Space Propulsion, Seville, Spain, 14-18 May 2018, SP2018_016

[8] F. Mier-Hicks, P. C. Lozano, *Thrust Measurements of Ion Electrospray Thrusters using a CubeSat Compatible Magnetically Levitated Thrust Balance*, 34th International Electric Propulsion Conference, Hyogo-Kobe, Japan, 4 July 2015, IEPC-2015-148, ISTS-2015-b-148

[9] W. Buckel, R. Kleiner: *Superconductivity – Fundamentals and Applications*. Wiley-VCH, Second, Revised and Enlarged Edition, Weinheim, 2004

[10] J. Bardeen, L. N. Cooper, J. R. Schrieffer, *Theory of Superconductivity*, Physical review, Volume 108, Number 5, 1 December, 1957

[11] K. Fossenheim, A. Sudbo, *Superconductivity - Physics and Applications*, Wiley, 2004